

BUCKLING AND POSTBUCKLING ANALYSIS OF SHELLS UNDER QUASI-STATIC AND DYNAMIC LOADS

R. Degenhardt, H. Klein, A. Kling, H. Temmen, R. Zimmermann
DLR Institute of Structural Mechanics
Lilienthalplatz 7, 38108 Braunschweig

1. INTRODUCTION

Thin-walled fuselage structures, partly subjected to compression and shear (torsion), are endangered by buckling. Present design procedures rest upon non-conservative conditions as to dynamic loading, e.g. landing impact, and on too conservative assumptions, if buckling due to quasi-static loading is considered.

With dynamic loading like landing impact a distinction should be made between relatively short and long, quasi-static loading durations, and loadings the durations of which are in the order of the longest lateral period (lowest eigenfrequency) of the structure. A particular problem is to be expected under the later loadings where the interaction of loading dynamics with the dynamics of the buckling process may lead to substantially reduced dynamic buckling loads, as compared with the buckling loads predicted by quasi-static loading. This load reduction actually is not considered in the design process. In order to overcome that problem, a fast and reliable simulation procedure has to be developed.

With buckling due to quasi-static loading, experiments have shown that the potential exists for further weight savings with stiffened composite structures by allowing postbuckling of the skin to occur during operation. Proper design enables the structures to act far within the postbuckling regime without any damage. This demand requires the development of an appropriate fast and reliable simulation procedure.

2. POSTBUCKLING OF CFRP STRUCTURES UNDER QUASI-STATIC LOADS

The structural behaviour of undamaged thin-walled stringer stiffened CFRP fuselage structures loaded in compression is primarily limited by its buckling and postbuckling performance. Extensive nonlinear finite element analyses are conducted and finally verified with two in-house tests. Based on this sound database a concept for a fast and reliable postbuckling algorithm is developed.

2.1 Numerical simulation

To analyze the pre- and postbuckling behaviour of stringer stiffened panels and cylinders the commercial nonlinear finite element tools ABAQUS/Standard and ABAQUS/Explicit are employed, and substantial investigations are undertaken with respect to the FE-model, the analysis procedure and finally the verification utilizing experimentally extracted data.

Stringer stiffened panel

Preliminary examinations are conducted, to ascertain the use of an appropriate shell element, the necessary mesh refinement and the stringer-skin connection. Finally a four-node shell element (S4R) with a side length of approximately 4 mm is employed to discretize the panel.

This relatively fine mesh is mandatory to include all kind of local and nonlinear effects in the analysis. Figure 1 depicts a clipping of the FE-model and some detailed information with respect to the stringer-skin connection. The adhesive joint is modelled using rigid elements (shown as straight lines connecting corresponding nodes of the skin and stringer elements). A slightly refined mesh is utilized as a

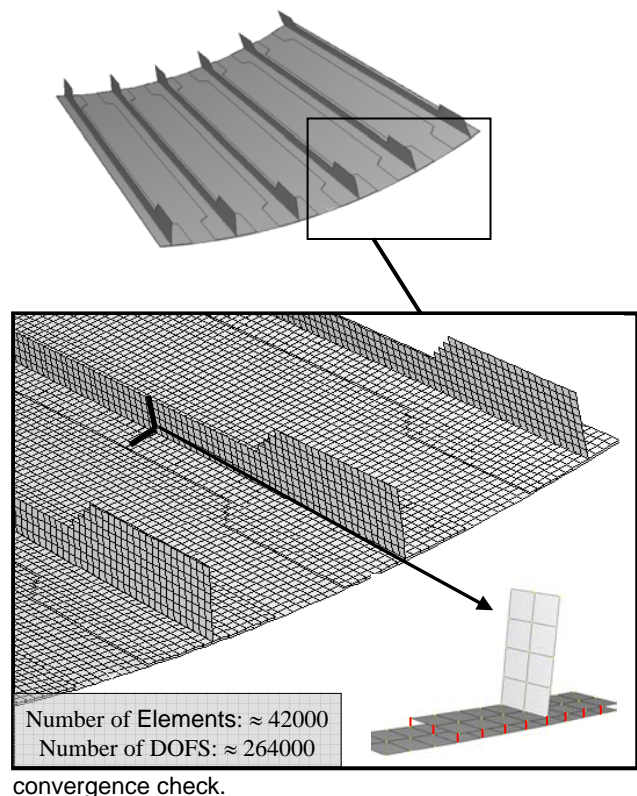


FIGURE 1. Finite element model with detailed stringer-skin connection

The approach to conduct the FE-analysis in ABAQUS/Standard consists basically of four stages (Figure 2): The preprocessing using e.g. MSC/PATRAN, a linear eigenvalue analysis (*BUCKLE) to extract buckling modes. These modes are used in the subsequent nonlinear analysis as scaled "artificial" imperfections. In contrast the results due to the optical digitizing of the skin (measured initial imperfections of the unstressed panel) can be used as "real" imperfections of the panel. In the nonlinear analysis with ABAQUS/Standard the built-in Newton-Raphson technique with adaptive/artificial damping (*STATIC, STABILIZE) is utilized. Finally the desired results (e.g. deformations, strains) are extracted with a postprocessing software (ABAQUS/Viewer).

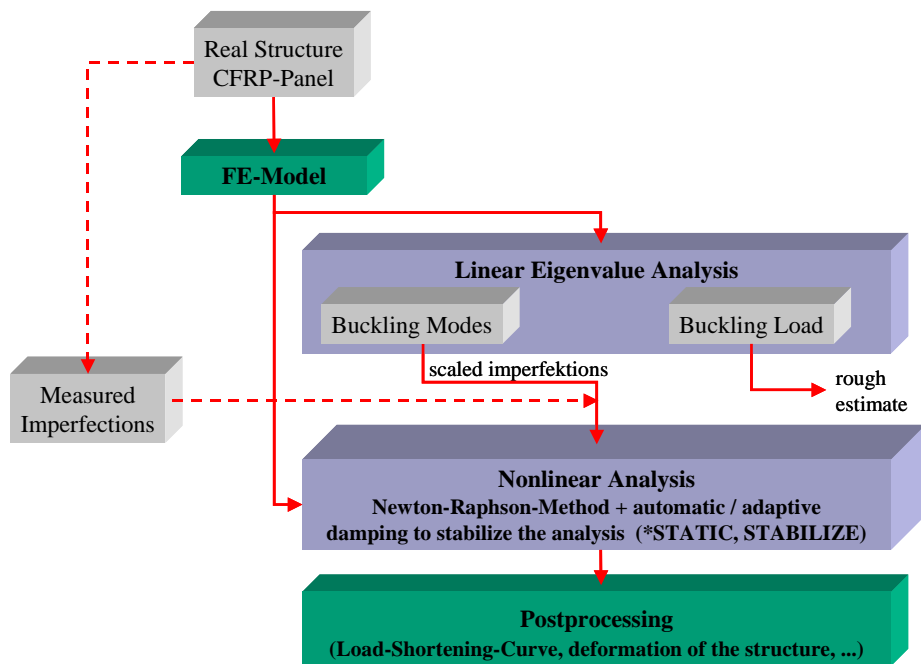


FIGURE 2. FE-analysis procedure in ABAQUS/Standard

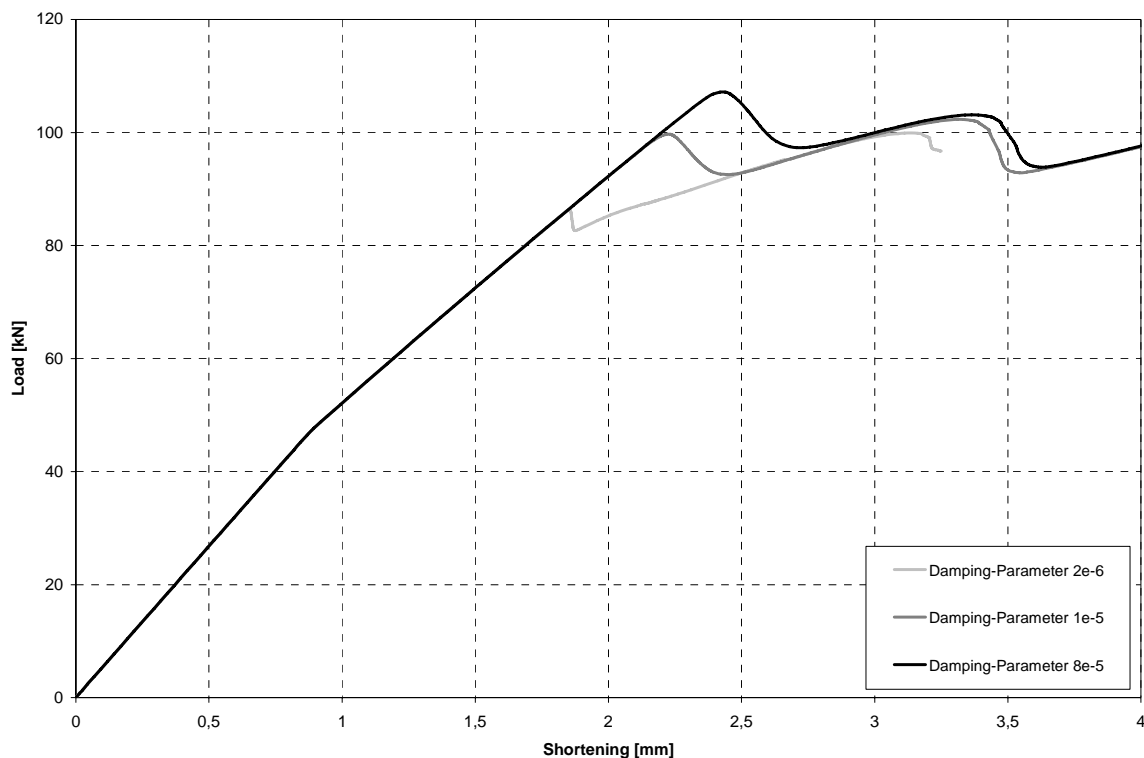


FIGURE 3. Influence of the damping-parameter in the analysis using ABAQUS/Standard

This solution method proved to be very stable for the considered structures. Several parametric studies are conducted to examine the influence of specific parameters in the nonlinear analysis.

Exemplarily the effect of the user-defined damping-parameter on the load-shortening curve is depicted in Figure 3. Detailed information on the examined panel can be found in Figure 6. It can be seen that an oversized damping value (e.g. 8e-5) will lead to an overestimated

load carrying capacity in the postbuckling region. Therefore the lower bound (here $2e-6$) has to be preferred by the user conducting several analyses.

Stringer stiffened cylinder

The approach, which is used to discretize and analyze stringer-stiffened CFRP cylinders, is similar to the practice, which is described in detail for the panel in the last section. Additionally several calculations are conducted with ABAQUS/Explicit under pure axial and torsion loading. Figure 4 and Figure 5 show the load-shortening curves with characteristic deformed plots of the cylinder (Radius=400 mm, Length=740 mm; 18 Stringer).

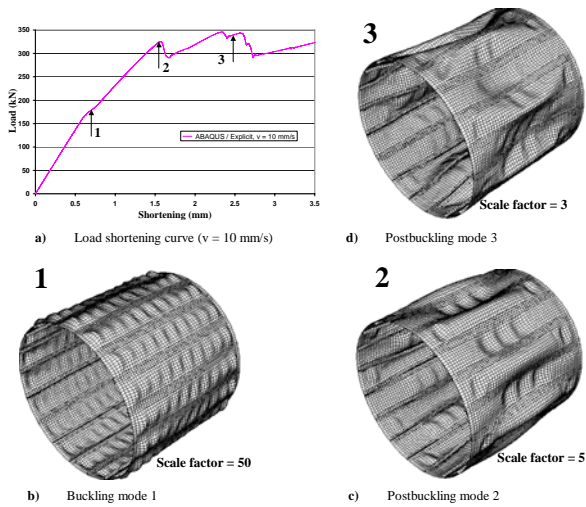


FIGURE 4. Pure axial loading

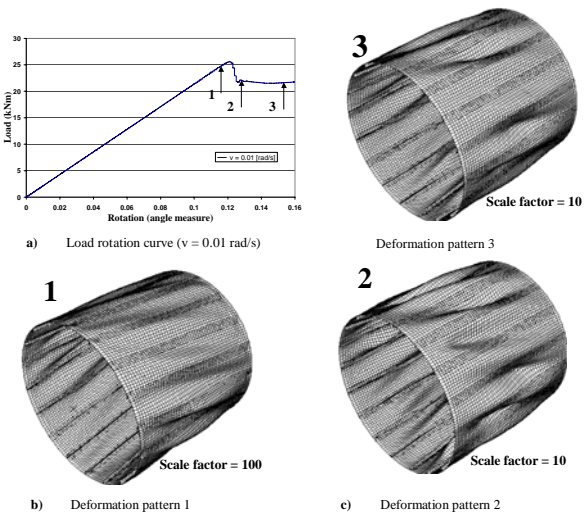


FIGURE 5. Pure torsional loading

2.2 Experiments

Two CFRP panels of nominally identical type and material (Hexcel, 6376C-HTA(12K)5-35%) have been manufactured. Figure 6 displays the panel and its basic dimensions.

The six T-shaped stringers have been manufactured separately, using a symmetric stacking sequence of prepreg material, and have been subsequently bonded to the skin. Ultrasonic tests have been conducted to ensure

the quality of the panels, especially the bonding between skin and stringer-flange. Figure 7 depicts the flaw echo of a panel where almost no in-homogeneity in the lamina as well as at the stringer-skin interface can be found.

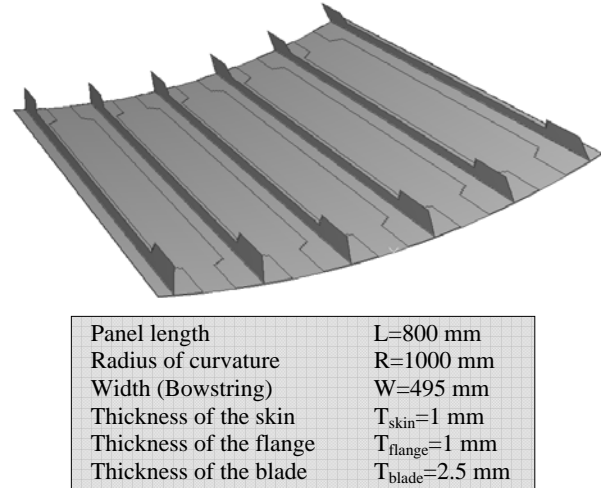


FIGURE 6. CFRP panel

Figure 8 shows the buckling test facility with one of the panels installed. A significant amount of sensors are used to extract local strains as well as axial and radial displacements. The displayed detail of the panel in Figure 9 depicts the chains of strain-gauges, which are utilized to determine local skin buckling (load and wave length). In addition, an optical measurement system is used to capture digital images of the deformed panel. After post-

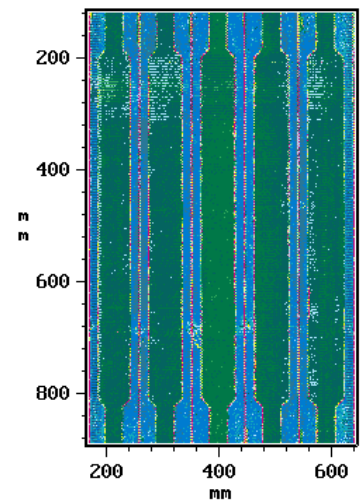


FIGURE 7. Ultrasonic flaw echo

processing of these images, which are made at 140 load levels during the experiment, the displacements at nodes of a fine optical mesh (representing the surface of the panel) are obtained. Using this relatively new optical system a quantitative comparison between the experimentally extracted deformation pattern and the numerically (FEM) calculated displacement is possible.

The diagram in Figure 10 shows the load-shortening-curves, which are scaled with respect to the corresponding loads and shortenings at the points where skin buckling occurs. In Figure 11 the measured strains of five strain gauges are depicted with respect to the scaled shortening. The occurrence of local skin buckling is associated with a small change in the stiffness of the test specimen. This

point is marked with an arrow in Figure 10. In accordance, the measured strains in Figure 11 start to diverge from their linear prebuckling path due to the sinusoidal deformation of the skin in axial (loading) direction. At a scaled shortening of approximately 1.9 a global non-symmetrical buckle emerges, which can be either seen by the sharp bending in the load-shortening-curve (Figure 10) or by the significant change in the local strains (Figure 11).



FIGURE 8. Buckling test facility



FIGURE 9. Panel with strain-gauges

The maximum load carrying capacity of both test specimens is reached at a factor of 1.95 times the buckling load, followed by a significant loss due to a sudden change in the postbuckling deformation towards a global symmetric buckle. This large (high energy) shifting results in a first failure of the structure – a local separation of the skin and the stringer-flange. Both experiments show good agreement and generate a detailed and reliable foundation to verify the nonlinear finite element analysis.

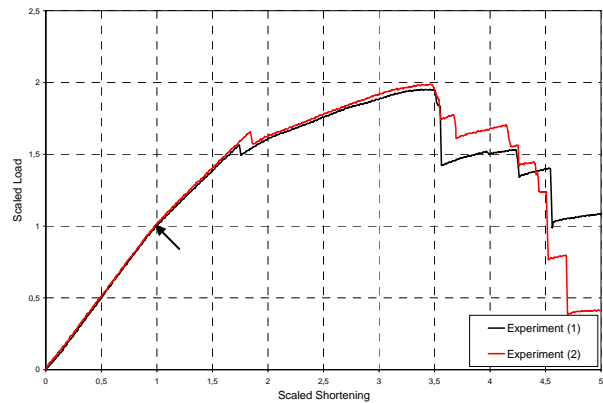


FIGURE 10. Load-shortening-curves

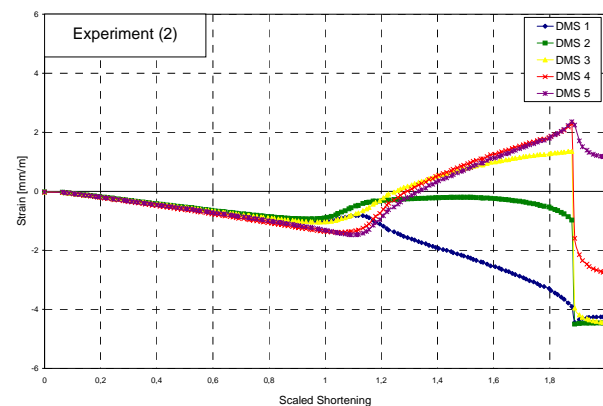


FIGURE 11. Local strains from strain-gauges

2.3 Validation of the numerical results

The diagram in Figure 12 shows that the numerical results match well with the experimental data – the axial stiffness in the pre- and postbuckling region, the occurrence of the sharp bending (global buckle) and the run of the curve up to first failure. The three pictures of the panel provide an idea how the deformation patterns appear at different stages in the postbuckling region.

Also the experimental deformations, determined with the optical measurement system, are very similar with respect to the postbuckling patterns (e.g. “local” skin buckling) gained by the nonlinear finite element analysis, cf. Figures 13 and 14. The number of buckles in axial/loading direction are identical in both figures.

In order to resume, the verification with reliable experimental data show the high quality of nonlinear finite element analysis along the whole postbuckling path up to first failure.

2.4 Concept of a fast and reliable postbuckling algorithm

An extensive literature survey with respect to a fast and reliable simulation procedure, analyzing the postbuckling behaviour of stringer stiffened fiber composite panels, has been conducted. A finite element model is used to extract a small number of “shape functions”, which can be utilized subsequently to analyze the structural behaviour. To reduce the error during the incremental nonlinear analysis the shape functions are updated regularly as shown in Figure 15, based on a predetermined error limit.

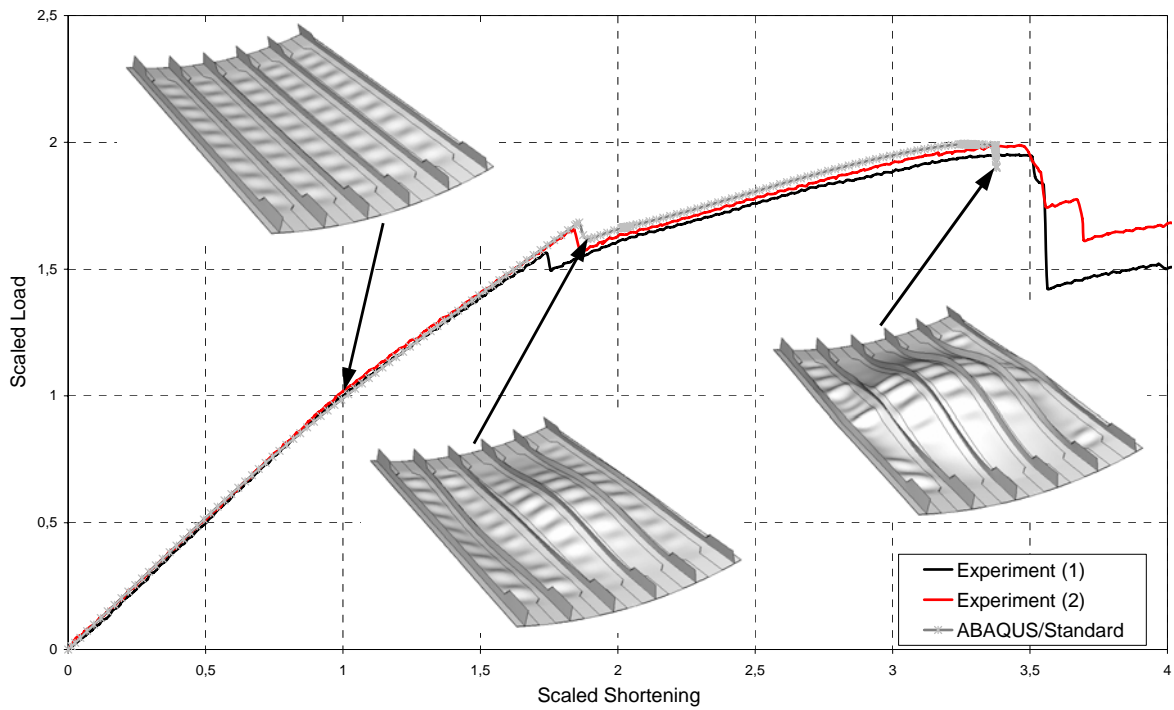


FIGURE 12. Load-shortening-curves (FE-analysis / experimental data)



FIGURE 13. FEM deformed plot

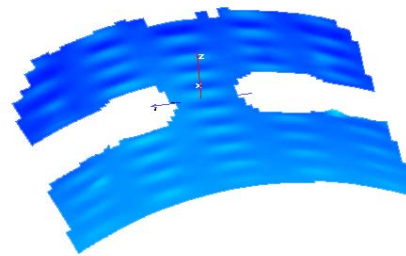


FIGURE 14. Optical measured deformation

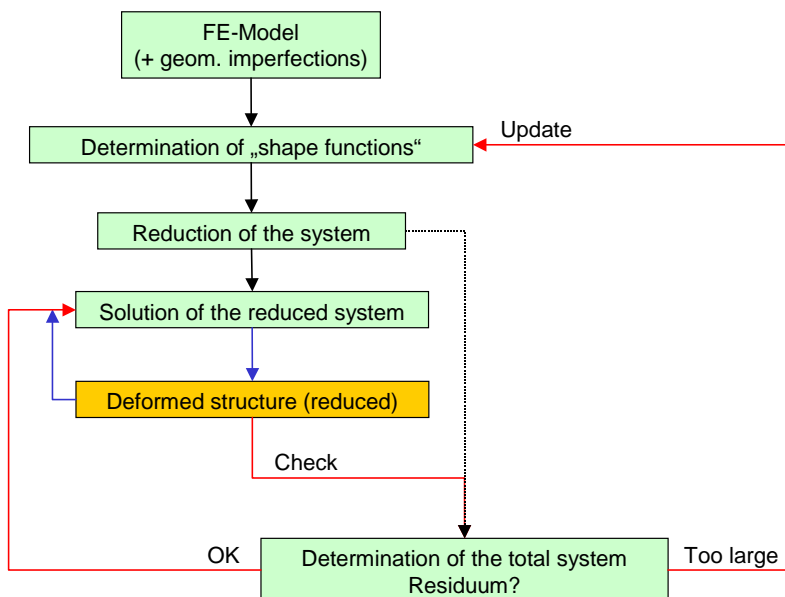


FIGURE 15. Concept of the postbuckling algorithm

3. BUCKLING BEHAVIOUR OF DYNAMICALLY LOADED CFRP CYLINDRICAL SHELLS

In the design process of dynamically loaded fuselage structures the quasi-static buckling load is presently the relevant buckling criterion. It is based on the not generally valid assumption that a dynamic process increases the buckling load. Under impulsive loads, such as landing impact of aircrafts or gust loading, the resulting buckling load can become lower in comparison with the quasi-static buckling load. In contrast to the current practice this critical dynamic behaviour - the reduction of the critical loads and displacements - must be taken into account in a safe design.

Even for isotropic shells the buckling under impulsive loads is hardly explored. Systematic investigations to understand the critical dynamic behaviour cannot be found in the literature, and analytical descriptions are missing due to the non-linear and transient nature of the problem. Because of the missing fundamentals systematic examinations in the dynamic regime have been carried out with help of FE parametric studies. The goal of the studies of axially compressed cylindrical shells under impulsive loads is to understand the dynamic buckling mechanism, to work out the influence of important parameters, to get data for the definition of test shells, and to provide the experimental verification. The existing FE tools are able to model dynamic buckling only with a very time consuming calculation. Therefore the development of fast and reliable design tools is a further important goal of these studies.

3.1 Numerical simulation

The commercial finite element tool ABAQUS is selected for the numerical simulation of the dynamic buckling. The studies of the transient non-linear dynamic are done with ABAQUS/Explicit, while ABAQUS/Standard is taken for the preliminary examinations (frequency and buckling analysis). In ABAQUS the three-dimensional shell elements S4R and S4RS are suited to model the dynamic buckling, however the element S4RS is available only in ABAQUS/Explicit. To get a consistent modelling the element S4R is chosen for all investigations. To facilitate and to accelerate the parameter variations in the model a parametric INPUT-FILE is written, which generates automatically a mesh. Therefore a preprocessor for the modelling is not necessary.

The numerical calculations have been carried out for unstiffened CFRP cylindrical shells with four layers. A fixed geometry - length = 510 mm, radius = 250,25 mm and total thickness = 0,5 mm - and different layer configurations are chosen. First, preliminary examinations (studies of convergence and calculation time to determine the mesh density, computation of frequency response and quasi-static buckling behaviour of the shells) are performed. Then, selective parameter variations are used to study the transient non-linear dynamics.

Preliminary studies

In addition to the knowledge of the frequency response (transversal bending modes, longitudinal axial mode) also the quasi-static postbuckling behaviour (the load displacement curve with buckling and postbuckling load and the corresponding buckling pattern) is necessary to

properly choose the parameters in the non-linear dynamic studies, and to interpret the dynamic buckling behaviour.

With an ordinary frequency analysis in ABAQUS/ Standard the stationary, coupled problem is solved. Transversal and longitudinal modes occur simultaneously in the frequency analysis, thus ABAQUS/Explicit is used to determine the frequency of the axial mode: A pulse load is brought to the shell to excite the axial mode and then the frequency of the arising mode is counted in the history diagram of the reaction force. The frequency of the lowest axial mode is generally higher than the frequency of the lowest bending mode.

ABAQUS/Standard and Explicit are used to perform the quasi-static postbuckling analysis. In ABAQUS/Standard the introduction of an imperfection and a stabilising damping is necessary to avoid convergence problems in the postbuckling regime. In ABAQUS/Explicit convergence problems don't appear, but the calculation time increases considerably in the quasi-static limit. The postbuckling of an axially compressed, unstiffened cylindrical shell is marked with a considerably reduced postbuckling load and a typical postbuckling pattern.

In any case, modelling with 240 knots in circumferential direction and 40 knots in longitudinal direction is used.

Parameter variation

The results of the preliminary examinations serve as a reference for the following investigations of dynamic buckling behaviour and influencing factors. In particular, investigations of different layer configurations, different loading conditions (linear and ramp like loads, boundary conditions with prescribed force and displacement) and the influence of the axial wave propagation on the critical dynamic behaviour have been carried out.

In the case of linear growing loads the well known increase of the critical loads could be calculated. But under suitable conditions with ramp like dynamic loads, both for prescribed displacements and forces, a reduction of the critical loads and displacements could also be shown. In a prescribed ramp like load the displacement u / force F is raised up to a maximum value within the ramp time T . Then this value is hold fixed.

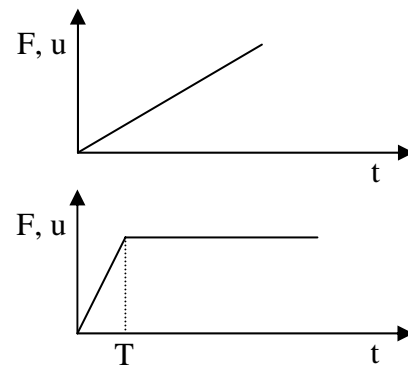


FIGURE 16. Load-history - linear and ramp like curve

Concerning the buckling load, both types of boundary conditions - prescribed displacements and prescribed loads - show similar results. However, in the case with prescribed displacements the results can be interpreted much better, since - in contrast to the case with prescribed

forces - the cylindrical shell forms a closed system with constant total energy. The buckling with prescribed displacements is defined as a transition to the postbuckling state, while the buckling with prescribed forces is marked with collapse like behaviour because of a continuously increasing energy.

In the studies with prescribed ramp like forces the orientations of fibres in four layers are varied. In Figure 17 the critical dynamic buckling load as function of the chosen ramp time and for different laminates is given. For a given ramp time the minimum load, at which a collapse like behaviour within an even very large time interval occurs, is defined as critical dynamic buckling load. For ramp times shorter than 1 ms a clear reduction of the buckling load is recognizable, while the values for long ramp times approach the quasi-static value. The critical dynamic behaviour is very pronounced for +24/-24/+41/-41 and +75/-75/+75/-75 laminates.

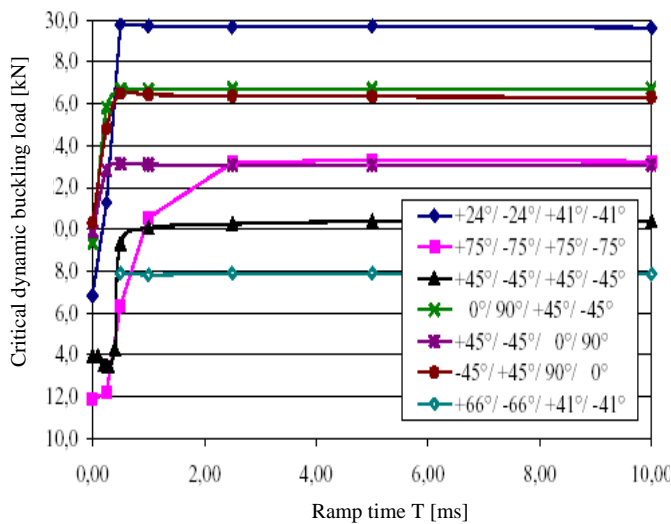


FIGURE 17. Critical dynamic buckling loads as function of the chosen ramp time, and for different laminates

The laminate +24/-24/+41/-41 is selected for studies with prescribed ramp like displacements to explore the mechanism of critical dynamic buckling. By reducing the maximum displacement at a given rise velocity the buckling occurs later. The critical dynamic displacement is defined as smallest displacement at which buckling still occurs. For the rise velocities 100 mm/sec, 200 mm/sec and 1 m/sec the critical dynamic displacement and the corresponding buckling loads take values of 0.44 mm and 31.4 kN, respectively. These values are comparable to the quasi-static buckling values. In Figure 18 the histories of the displacement and the reaction force for a rise velocity of 100 mm/sec are given.

For a given rise velocity of 2 m/sec the calculations yields a reduced critical displacement of 0.33 mm, and the corresponding critical buckling load takes a value clearly below 30 kN, as can be seen in Figure 19. However, since the axial forces oscillate substantially in the dynamic regime, the buckling loads can be determined only approximately. Depending on the definition of buckling load, the value of the dynamic buckling load is given by a value between 22,5 kN and 25 kN. Increasing the rise velocity leads to a further reduction of the dynamic

buckling load. As shown in Figure 2, the minimum of the dynamic buckling loads is 17 kN, a value between the quasi-static buckling load of 31.4 kN and the postbuckling load of 8 kN. The necessary ramp time to observe a critical dynamical behaviour is determined by the characteristic time of the axial mode of 0.3 ms. In comparison the characteristic time of the lowest bending mode is 4 ms. The evaluation of the calculations in the critical dynamic regime leads to the following results: At the beginning the ramp load excites an axial force wave in the cylindrical shell. After a time comparable to the characteristic time of the bending mode the energy of the high frequency axial mode is converted by mode coupling into energy of the bending waves. Within this time interval the system has sufficient time to relax, which means that the amplitude of the axial oscillations becomes essential smaller. The transition in the postbuckling state follows with a delay of time, which is again comparable to the characteristic time of the bending mode. The value of the dynamic postbuckling load corresponds to the quasi-static value of 8 kN.

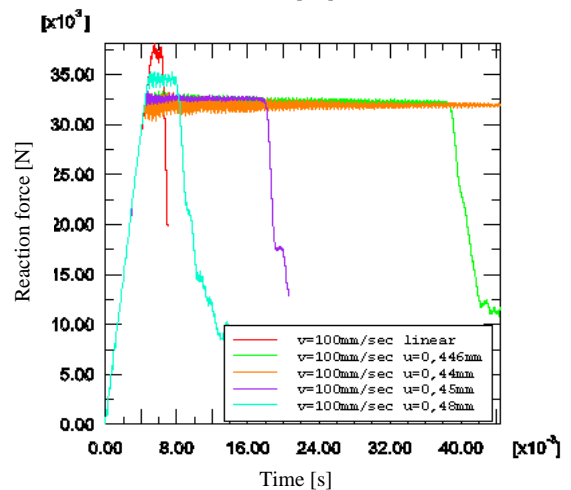
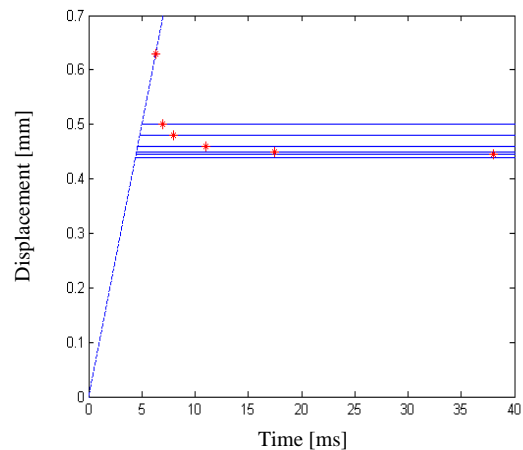


FIGURE 18. Time history of the displacement and the reaction force for different maximum displacements and for a rise velocity of 100 mm/sec. A red asterisk in the displacement history indicates a buckling event. Laminate:+24/-24/+24/-24.

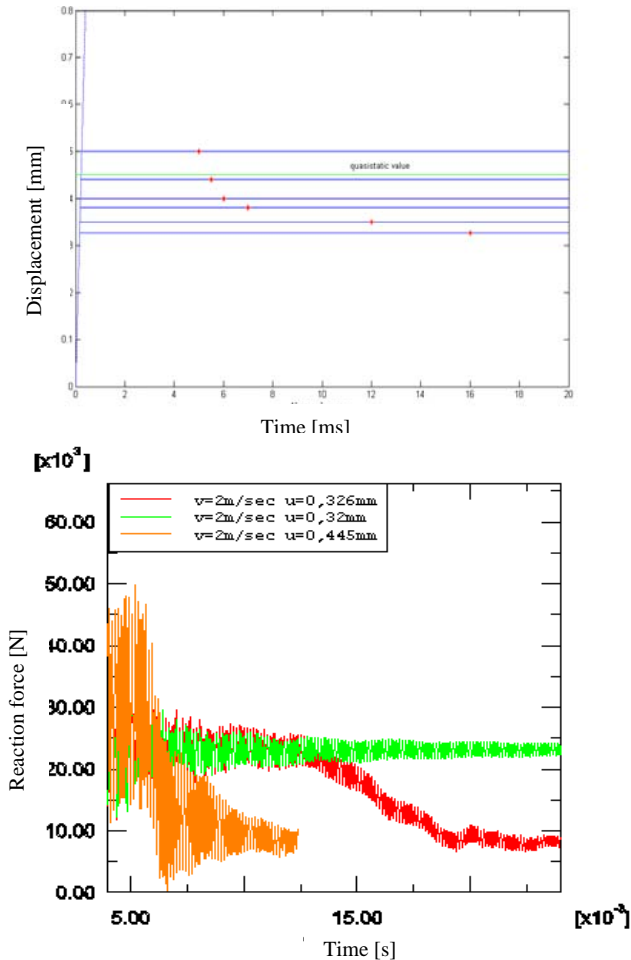


FIGURE 19. Time history of the displacement and the reaction force for different maximum displacements and for a rise velocity of 2 m/sec. A red asterisk in the displacement history indicates a buckling event. Laminat:+24/-24/+24/-24.

To explore the influence of the in-plane wave propagation, the FE-model is expanded with help of Connector Elements. These elements model damping forces, which depend on the velocity between the knots. With a suitable choice of the damping parameter the amount of the axial oscillations and the critical dynamic effect decreases considerably.

The presented numerical parametric studies of perfect, dynamically loaded cylindrical shells indicate, that the occurrence of a longitudinal axial mode and its coupling with a bending mode is necessary to get critical dynamic behaviour. In contrast to this result, up to now it was assumed that the ramp time has to be comparable to the characteristic time of the bending mode. The frequencies of the axial waves are much higher than the frequencies of the bending modes. This fact delivers new aspects for the experiment, the theory and the application; the consequences must be explored. In the critical dynamic regime the value of dynamic buckling load is given by a value between the quasi-static pre- and postbuckling load.

3.2 Experiments

Experimental verification is indispensable to control the numerical results. Because of lack of literature, the

reliability of the numerical result cannot be presupposed. In addition, not all factors (such as the influence of damping and imperfection), can be considered in the beginning of the numerical studies; the experiment would be helpful to fix some unknown factors. Thus dynamic buckling tests are needed.

In quasi-static tests already there are great demands on the experimental technology, which in particular are related to introduction of loads as perfect as possible into the thin-walled shell. Thus the use of the buckling test facility at the DLR Institute of Structural Mechanics is obvious. The facility, however, had to be equipped with a new hydraulic system because of the high dynamical demands. As a typical case of loading the landing impact of an aircraft was assumed. At first the structure is subjected to quasi-static initial load. The impact itself is divided into phases of acceleration, loading and retardation on a high load level.

The buckling test facility is equipped with a hydraulic cylinder controlled by two servo-valves, a two-stage one for quasi-static loading up to the initial load and a three-stage one for the actual impact. The port apertures of their oil flows are controlled separately, each by a control voltage. At the two-stage valve the velocity of the actuating piston nearly is proportional to the control voltage. At the three-stage valve the control piston of the third stage is moved by the oil flow of the second one. Its velocity therefore is proportional to the voltage, too. The third stage piston opens the aperture of the oil, which controls the velocity of the actuating piston. Thus its acceleration would be adapted nearly proportional to the control voltage. This property requires the position of the third stage piston to be controlled proportional to the valve voltage by an additional inner loop of a cascade. Thus the velocity of the actuating piston again is proportional to the control voltage like at the two stage valve. The control properties of the three-stage valve, however, become very complex at high dynamics, and are hardly predictable.

Hydraulic cylinder and servo-valves with the required properties at the limits of feasibility are special designs. Thus at the beginning of the development there was own experience only with two stage servo-valves and the assumptions of the manufacturer. Such a hydraulic cylinder usually is operated in a closed-loop control system. In this case with two valves also two loops are necessary. Such a servo-loop compares a given value (set point) with the realised control signal (actual value: load, displacement, e.g.) (see Figure 20). The set-up error is used to move the actuating piston in that way, that the actual value is adapted to the set point. The set-up error so disappears. As a complete test sequence with different load phases shall be controlled, an additional pulse control loop is needed, the trigger points of which depend on the actual value, too.

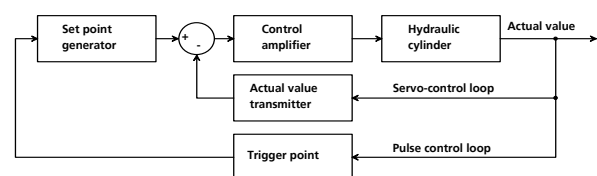


FIGURE 20. Control loop of the hydraulic cylinder

Operating with a low dynamic level, such a system is known for its great accuracy and non-problematical

behaviour. With a higher dynamic level the delay in the system exerts more and more influence. As it is mentioned before, that a set-up error is required to move the actuating piston, this error gets an inadmissible size. On top of this is the already mentioned complex control behaviour of the three-stage valve. The preparatory tests proved, that a closed servo-control loop is not suitable with a three-stage valve for the real impact. An open loop, however, is not able to react on the actual system response. Therefore the system response on the signal of the set point generator has to be predictable exactly to consider the system performance in the adjustment of the set point.

By the assumptions of the manufacturer a rectangular pulse of the set point should result in a ramp with constant velocity and on the decreasing flank the same into the opposite direction, while the corners of the response function are rounded smoothly because of the acceleration. This would correspond with the load profile of a landing impact. The amplitude of the set point as a measure for the impact velocity and the rectangle width for the impact amplitude would be controllable easily by the trigger of the pulse control loop. But it was simply to be regarded during the first tests, that the assumed behaviour did not correspond to the real system response (see Figure 21).

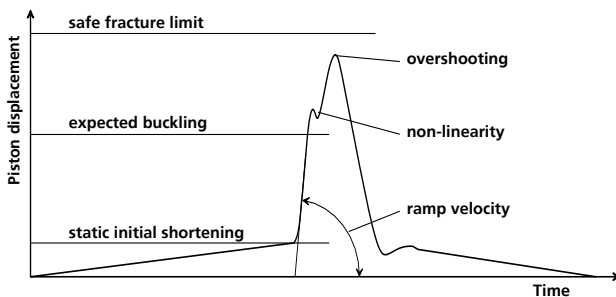


FIGURE 21. Response on a rectangular pulse

The actuating piston responds nearly linearly to the pulse of the valve voltage. But then the behaviour turns into an intense non-linearity, resulting from the interaction between the three stages of the valve and the inner control loop. Shape, position and size of the non-linearity depend on the valve voltage. The overshooting is so high, that exceeding of the safe fracture limit of the test specimen only can be avoided, if the trailing edge is triggered before the piston starts moving. That means, that controlling of the phases of the pulse by a trigger signal is not possible. Thus the pulse control loop has to be opened, too.

Now the three-stage valve is controlled directly without any loop, while the two-stage one continues to work in a servo-control loop and in a pulse control loop. The handling of the control sequence is complicated and can only be automated up to a certain point, because the expected buckling has to be placed before the non-linearity, and the overshooting must have a safe distance to the fracture limit. At the same time the demanded loading velocity has to be met. Parameters of adjustment are amplitude and width of the rectangular valve voltage. For that purpose the complete characteristic field of the hydraulic cylinder and servo-valve combination is picked up, and a software is developed, which supports the decision on the adjustment parameters by the user. The

facility is ready for pulse tests and shows a distinct stable behaviour for such a high level of dynamics.

3.3 Development of fast analysis tools

To describe the dynamics of shell buckling usual analytical approaches and simple FE shell models neglect the influence of the high frequency in-plane mode. A stress function is introduced to realize this equilibrium condition mathematically. These approaches yield very efficient calculation tools in the low frequency regime, however they are not suitable for the description of the critical dynamic behaviour. The numerical integration of complex shell models, which also consider the axial mode, requires a clearly increased amount of calculation. Additional dynamic degrees of freedom have to be integrated and the number of time steps increases, since the width of the time step is directly influenced by the high frequencies of the axial wave. Thus a complete solution of the non-linear and transient problem doesn't lead to a fast analysis tool. In a design process only the lowest critical loads and displacements are of interest. Taking this fact into account a complete solution of the problem does probably not become necessary. Because no fast design procedure for dynamically loaded shells is found in the existing literature, the development of new methods is necessary. A first approach, which is based on the linear stability theory, and in which the axial mode is taken into account, is imaginable. The contents of information from such a linearized approach have to be analyzed.

4. SUMMARY

Numerical simulations of the buckling and the geometrically highly non-linear postbuckling behaviour of CFRP curved panels and cylinders under quasi-static loading, based on the FE method, are performed. For curved panels the numerical results are in excellent agreement with results obtained by physical tests, whereas for cylinders testing was not carried out. However, the lessons learned for panel simulation are also valid for cylinders, in particular, as with cylinders no influence of lateral edges has to be taken into account. With the FE simulations the computing time is extremely high, and development of fast procedures for use in the design stage is desirable. A concept for such a procedure based on regularly updated shape functions is established.

Development of fast procedures is also a need for the simulation of the buckling behaviour of dynamically loaded fibre composite shells. However, this is a more fundamental topic than that of postbuckling; and the phenomenon of critical interaction leading to buckling load reduction, which is of basic importance for the development of appropriate fast simulation procedures, was not understood well. Therefore a multitude of time consuming parametric FE simulations are conducted. The results indicate, that the occurrence of a longitudinal axial mode and its coupling with a bending mode is the physical pre-condition for critical dynamic behaviour. Based on this insight, a concept for the development of a fast procedure is generated. The buckling test facility is made ready for tests with impulsive loading by application of a new hydraulic system and the development of its necessarily complex control.